Journal of Modern Optics
Vol. 55, No. 1, 10 January 2008, 55–66

Taylor & Francis
Taylor & Francis Group

Light driven self-ordering in fused quartz

B. P. ANTONYUK*†, A. Z. OBIDIN‡, S. K. VARTAPETOV‡ and K. E. LAPSHIN‡

†Institute of Spectroscopy, Russian Academy of Science, 142190 Troitsk, Moscow Region, Russia
‡Physics Instrumentation Center, General Physics Institute, Russian Academy of Science, 142190 Troitsk, Moscow Region, Russia

(*Received 20 November 2006; in final form 14 February 2007*)

Theoretical and experimental investigation of self-ordering in a fused quartz under strong light pumping is presented. It is shown that uniform radiation drives a self-organization process in a random medium and macroscopic spatially ordered structure is formed.

1. Introduction

Ordering of a matter by light is achieved in two ways. First there is production of some spatial profile of the light intensity acting on a sample and transmitting the profile to the sample. We refer to the method as 'forced' ordering going forward, and there are a lot of examples of such ordering of a matter using different masks or wave interference in order to create the light intensity profile of a proper form.

Second, which is the subject of the present paper, involves a process of self-ordering under spatially uniform radiation. We paid special attention to form a homogeneous light beam and observed spatial ordering in fused quartz caused by light of constant intensity over the investigated region of the sample. A simple trick was used in order to check that homogeneous radiation induces the ordering: the sample was moved back and forth perpendicular to the light beam during preparation of the state. Ordered structure obviously would be smoothed by the sample motion if it is prepared in the frame of the above-mentioned first approach when the light intensity profile prints a corresponding profile in the matter. To the contrary, the sample motion has no effect on the monitored region of the sample if radiation is homogeneous and the prepared structure is not influenced by the motion. We experimentally confirmed the fact: our light induced structure does not depend on the sample motion, therefore we can state definitely that it is produced by the homogeneous light field. New structure was visualized in an ablation process. It was

*Corresponding author. Email: antonyuk@isan.troistk.ru

Journal of Modern Optics
ISSN 0950–0340 print/ISSN 1362–3044 online © 2008 Taylor & Francis
http://www.tandf.co.uk/journals
DOI: 10.1080/09500340701281251

observed in diffraction of the probe He–Ne beam and in the microscope. Measurement of the diffraction angle allowed us to find the period of the light-induced structure, which turned out to be equal to $2 \pm 0.2\,\mu m$. This measurement was confirmed by microphotograph. It is worth noting that the deeper the ablation crater is, the more perfect the structure that is prepared which might be observed in the narrowing of the diffraction peaks or visually in the microscope.

We mention one more peculiarity of the self-organized system. The period of the newly formed structure had nothing in common with the light scales (light wavelength, coherent length, beam size etc.) so what would be the case if it were the forced ordering way. We performed about 10 preparations of the new structure using light beams with different coherent lengths, beam diameters and different beam power and found the same period $2\,\mu m$ in fused quartz which, according to theory, is determined by material characteristics, the main being the density of the trapped electrons. This feature is quite analogous to the behaviour of the violin string under constant motion of a fiddle stick. The latter excites the string vibration but the temporal period of the oscillation is determined by internal characteristics of the violin. The violin string motion presents an example of temporal self-organization under constant action and reveals a peculiar, for self-organized systems, feature—independence of the new period on the characteristics of the driven force.

The ordering discussed belongs to the class of self-organization phenomena in open dissipative systems. Typical examples of this class are the Benard convection [1], Belousov–Zhabotinsky reactions [2] and the Turing instability [3]. All self-organization phenomena are driven by some external flow through the system: heat in Benard convection, chemical reagents in Belousov–Zhabotinsky reactions, etc. The optical analogue of Turing instability was presented by Arecchi [4]. In this case light amplitude has been modulated in time and space, which was crucial for the organization to occur. Our investigations [5, 6] have shown that steady light flow through a system can provide ordering either. Such steady light is a driving force which bunches the electrons in the case in hand.

The reason for the light driven ordering discussed is the following. We show that strong light transfers electrons in random media predominantly opposite to the forces acting and particles pushed by light are gathered into macroscopic bunches. In order to explain this point we consider light driven electron kinetics in disordered matter. Electron spectra of a random medium consists of extended electron and hole bands divided by the 'gap'. The gap is filled by local states corresponding to the electrons trapped in local minima of an electron potential. Electron energy in the trap and trap positions are random. We consider the case when photon energy is less then the gap and light induces electron transitions between local states only. Electrons and holes in extended states are not generated in these conditions. Light driven as well as spontaneous transfers of electrons between the traps are taken into account.

An electron absorbing a photon gains energy and shifts from one trap to another with higher energy level (figure 1). For an electron located in initial trap i with the energy level $\varepsilon_i^{(0)}$ there is a corresponding absorption band with resonance at some excitation energy M (figure 2). The electron can be transported to any other trap f

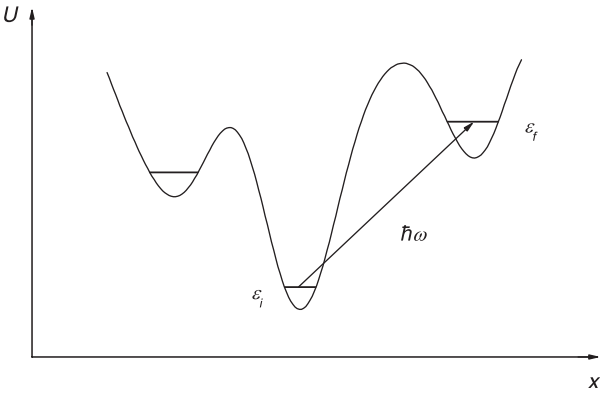

Figure 1. Electron transfer between different traps in a random medium.

with the excitation energy $\varepsilon_{fi} = \varepsilon_f^{(0)} - \varepsilon_i^{(0)}$ within the absorption band and all directions of transfer are equiprobable. Let us denote the transitions with the $\varepsilon_{fi} < M$ as low energy and these with the $\varepsilon_{fi} > M$ as high energy ones. Now we embed the other electrons at positions j, Coulomb interaction shifts all the initial trap energy levels for the first electron, hence shifting the excitation energies by $(e^2/R_{fj} - e^2/R_{ij})$, where $R_{fj} = |\mathbf{R}_f - \mathbf{R}_j|$ and $R_{ij} = |\mathbf{R}_i - \mathbf{R}_j|$. The directions of transfers are not equivalent any more: all the possible final states that bring the first electron closer to the second one (in opposite direction to the electric force) get higher excitation energy, among them low energy excitations shift closer to the resonance M (figure 2). The final states that would bring the electron in the direction of the electric force reduce the excitation energy and low energy excitations shift off the resonance. That is why low energy transitions of an electron are directed preferably against the direction of acting electric force (in the direction of increase of potential energy). High energy excitations go mainly in the opposite direction but these states have less lifetime in comparison with deep levels and therefore contribution of low energy excitations dominates. At high pumping these transitions dominate also over ordinary mobility which is quite low and independent of laser power.

2. Electron bunching under light pumping

A set of traps in our model are chaotically generated in space with a given average distance a and their initial energy levels $\varepsilon_i^{(0)}$ are randomly distributed in accordance with chosen densities of states. We start from the initial state where trapped electrons occupy low energy traps. Electrons 'feel' each other through the Coulomb interaction.

$$\varepsilon_i = \varepsilon_i^{(0)} + \sum_j e^2/R_{ij}, \tag{1}$$

where $R_{ij} = |\mathbf{R}_i - \mathbf{R}_j|$ is the distance between the electrons.

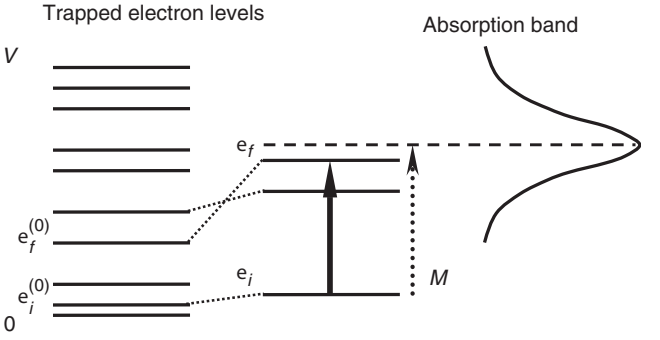

Figure 2. Light driven electron transitions between different traps. For transitions towards the other electron, the Coulomb contribution shifts low energy excitations closer to resonance.

The excitation energy for the electron transition from trap i to trap f is

$$\varepsilon_{fi} = \varepsilon_f - \varepsilon_i. \tag{2}$$

The probability rate w_{fi} for an electron to transfer from a trap i to a trap f depends on the energy difference $\varepsilon_{fi} = \varepsilon_f - \varepsilon_i$. If ε_{fi} is positive the only possible way for the transition is by absorbing a photon, the rate is given by [7]

$$w_{fi} = I\sigma_0 \cos^2\theta_{fi} \exp\left(-\frac{(\hbar\omega - \varepsilon_{fi} - A)^2}{\Delta^2} - \kappa_{fi}R_{fi}\right) \quad (\varepsilon_{fi} > 0), \tag{3}$$

where I is photon flux, $\hbar\omega$ is photon energy, θ_{fi} is the angle between $\mathbf{R}_{fi}$ and the light polarization vector, $\sigma_0 \approx 10^{-18}\,\mathrm{cm}^{-2}$, $\Delta \approx 10^{-1}$ to $10^{-2}\,\mathrm{eV}$, the factor κ_{fi} is determined by the degree of overlap of the wave functions of the initial and final states. The probability has a resonance at $\hbar\omega = \varepsilon_{fi} + A$, $A \approx 10^{-1}$ to $10^{-2}\,\mathrm{eV}$ is the Stokes shift and decays exponentially with transfer distance R_{fi}, $M = \hbar\omega - A$. Electron transfer given by formula (3) is phonon assisted. This fact designates two peculiar features of our system: it is dissipative (not Hamiltonian); phonons brake phase relations for the electron wave functions, therefore, nondiagonal elements of the density matrix vanish and only probabilities of the site populations appear in consideration. In the considered case of light driven and phonon assisted transitions at room temperature these probabilities give full and correct description of the system.

If the energy difference $\varepsilon_{fi} < 0$, the electron has more ways to transit. First, it can undergo light-induced transition, probability of the latter being described in a way very similar to (3) with the only change A to $-A$ [7]. Secondly, it may relax to the lower energy state with the rate

$$\gamma_{fi} = \gamma_0 \exp(-\kappa_{fi}R_{fi}).$$

So, for the electron transition process with the energy decrease we have

$$w_{fi} = I\sigma_0 \cos^2\theta_{fj} \exp\left(-\frac{(\hbar\omega - \varepsilon_{if} + A)^2}{\Delta^2} - \kappa_{fi}R_{fi}\right) + \gamma_0 \exp(-\kappa_{fi}R_{fi}) \quad (\varepsilon_{fi} < 0). \tag{4}$$

The factor γ_0 is of the order of magnitude of the inverse lifetime for excited electron states in an atom, so that $\gamma_0 \approx 10^8\,\mathrm{s}^{-1}$.

Wave function of the trapped electron outside the trap i is $\Psi_i(\mathbf{R}) \propto \exp(-\kappa_i|\mathbf{R}-\mathbf{R}_i|)$, where $\kappa_i = [(2m/\hbar^2)(V-\varepsilon_i)]^{1/2}$, m is the electron mass, V is spacing of bottom of trapped levels from the bottom of the extended states. Normal scale for this parameter is $\kappa_0 = [(2m/\hbar^2)V]^{1/2} \approx 10^7\,\mathrm{cm}^{-1}$. Wave function of deep levels vanishes rapidly outside the trap while shallow levels have long tails of wave functions. Their overlap is determined by the slowest function, therefore, $\kappa_{fi} = \kappa_0 * \min\{[1-(\varepsilon_f/V)]^{1/2},\ [1-(\varepsilon_i/V)]^{1/2}\}$ [5].

According to the above stated rules (1), (2), (3), (4) we examined the behaviour of a many-body system. The governed parameter of the theory is dimensionless pumping

$$\mu = \frac{I\sigma_0}{\gamma_0}. \tag{5}$$

The corresponding model is presented in detail in [5, 6]. Computer simulation of the electron kinetics in the finite sample in the external electric field shows that indeed electrons are transported by light predominantly opposite to the electric force direction (electric current flows contra to the voltage drop). As a result static polarization directed against the external electric field is established. This polarization amplifies the initial field and the process is stopped at the value of the field 10^5 to $10^7\,\mathrm{V\,cm}^{-1}$ (for details see [10, 11]). At the achieved field of saturation, light-induced transitions are in the dynamical equilibrium with contraflow due to the ordinary electron mobility.

The phenomenon discussed is observed in one-, two- and three-dimensional systems, therefore we also performed a computer simulation of the light driven electron kinetics for two dimensions, convenient for direct observation of electron spatial distribution and its motion. We calculated temporal behaviour of squared radius of the electron bunch

$$R^2 = 1/2\sum_{ij}|\mathbf{R}_i - \mathbf{R}_j|^2 \tag{6}$$

and its normalized Coulomb energy

$$V_\mathrm{c} = 1/2\sum_{ij}|\mathbf{R}_i - \mathbf{R}_j|^{-2}, \tag{7}$$

where $\mathbf{R}_i, \mathbf{R}_j$ are positions of the electrons. Without light pumping electron kinetics is slow and these functions show minor temporal change. Switching on the laser field causes fast kinetics and compression of the electron cloud. Its size R^2 drops (figure 3) and Coulomb interaction V_c is increased exhibiting the light driven electron bunching. This looks like omnidirectional light 'pressure' acting upon the electrons. This 'pressure' is different from Lebedev's light pressure. The last acts in the direction of the light beam and is proportional to the photon impulse $\hbar\mathbf{k}$. Our 'pressure' acts in all directions (to the centre of the blob) and does not depend on $\hbar\mathbf{k}$.

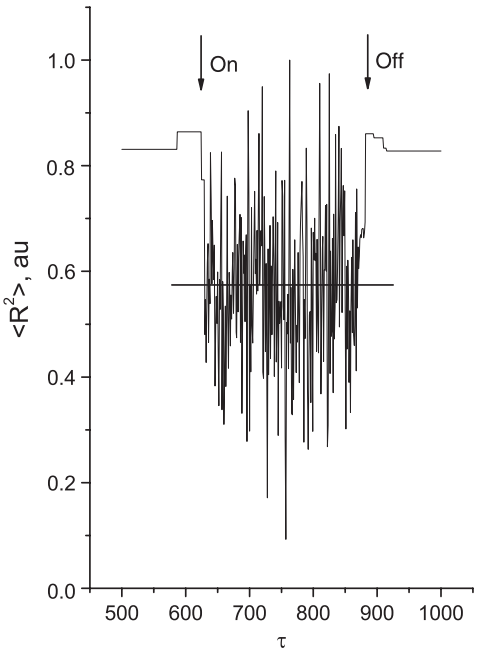

Figure 3. Light driven bunching of the electrons. Squared size of the electron cloud $\langle R^2 \rangle$ is decreased under light pumping (parameters are $a = 50\,\text{Å}$, $1/\kappa = 50\,\text{Å}$, $\mu = 100$, number of electrons $N = 10$).

Electron bunch formation results in increase of the static electric field which gains maximum at the boundaries of the bunches. Bunch size might be estimated from the electrostatic equation:

$$R = \frac{3}{4\pi} \frac{E}{n|e|}.$$

For electric field $E = 10^7\,\text{V cm}^{-1}$ and electron density $n = 10^{18}\,\text{cm}^{-3}$ we would expect micron size scale of the electron pattern: $R \approx 10^{-4}\,\text{cm}$. We see indeed that the new scale R does not depend on the scale of light field but is determined by internal properties of the matter and this is the peculiar feature of self-organized systems. Total charge of the bunch is 10^6 electrons. Taking into account that the electric field is $(charge)/(distance)^2$ and one electron generates atom field $E = 10^9\,\text{V cm}^{-1}$ at the atom distance $R = 10^{-8}\,\text{cm}$, we find that 10^6 electrons produce the electric field $E = 10^7\,\text{V cm}^{-1}$ at the distance $R = 10^{-4}\,\text{cm}$ (at the bunch boundary). This is a strong field but only a minor part of the available electrons have changed their states: 10^6 electrons compose only 10^{-5} part of the number of valence electrons in the volume of the bunch. So, this is a comparatively low level of excitation of the matter. The reason for this relatively soft excitation is long duration of the light pulses used in our experiment and calculations (20 ns). Another situation rises if femtosecond laser pulses are used. Peak power is higher in this case to a factor of about 10^5 and strong excitation of the matter takes place, discussed at the end of the

paper (section 4). As far as bunches are charged and therefore repulse each other we should expect that they will form spatially ordered structures analogous to Wigner crystal. This ordering was observed in the experiment presented below.

We used the strong electric field $E = 10^7\,\mathrm{V\,cm^{-1}}$ at the boundary of the bunches in order to visualize bunch structure of the prepared state. This field is near the damage threshold $E_\mathrm{d} = 3 \times 10^7\,\mathrm{V\,cm^{-1}}$ for our material and due to so high an electric field, the boundaries of the bunches become a weak chain in a network of coupled atoms. Atomic bonds may be broken much more easily at the boundaries revealing bunch structure. We used photons with the energy $\hbar\omega \approx 7\,\mathrm{eV}$ which is a little bit less than the gap $\approx 8\,\mathrm{eV}$ in our material. They are not absorbed by the main part of the sample (measurement shows that untreated sample absorbs about 10^{-3} part of photons passed) and only at the boundaries of the bunches, the lack of energy $\approx 1\,\mathrm{eV}$ an electron gains from the electric field $10^7\,\mathrm{V\,cm^{-1}}$ during tunnelling through a reasonable distance $10^{-7}\,\mathrm{cm}$ and an electron–hole pair in extended states is generated (Franz–Keldysh effect [8, 9]). The light driven bond breaking is site selective now and this local fusion reveals bunch structure of the self-organized state. We observed this bond breaking manifested bunch structure of the self-organized state in the regime of ablation: after laser treatment of the sample the ordered bubble surface corresponding to the maximum of the static electric field was observed.

3. Experimental

High quality fused quartz samples were used in our experiments. Before the experiment the samples had been subjected to ultrasonic cleaning in acetone and ethanol followed by washing in de-ionized water. The experimental set-up scheme for fused quartz ablation is shown in figure 4. The ArF excimer laser (193 nm, CL-7000, PIC GPI) was used. It generated 20 ns FWHM pulses with energies up to 350 mJ and pulse repetition rate up to 100 Hz. A laser beam was focused on the rear side of a sample by the lens made of MgF_2. Ablation was performed in ambient air. Surface morphology and etched structure depth were analysed with an optical microscope with further recording using a Cohu-4812 CCD camera. Normally the stable resonator for the ArF laser was used together with a homogenizer that enabled one to minimize the energy density distribution fluctuations (deviation from Gauss form is less than 2×10^{-2}) and also minimize spatial coherence of the beam. In some particular cases the unstable resonator was with the spatial coherence length not less than 6 mm in one direction—horizontal—of the beam cross-section and less than 10 μm in the vertical direction.

It is convenient to study output surface of the sample in the convergent beam. In this case the maximum of the light intensity in the sample is located at the studied surface and it is easy to provide a soft condition for the ablation. Study of the input surface is more difficult because below the treated surface light power is higher, therefore, optical damage takes place prior to ablation. In the first experiment we used a high quality fused quartz optical lens as a sample. The input surface of the sample was plane but the output surface was spherical (figure 4) so that the shift of

the sample perpendicular to the beam axes changed the angle between the beam axes and the treated surface.

As can be seen in figures 5–9 the material sputtering (ablation) occurs on the rear side of the sample with no stimulation of the process (such as plasma generation in the vicinity of a sample or specific UV absorbing medium as used in [12]). The process starts itself at the upper threshold laser fluence level ≈ 5.5 to $6\,\mathrm{J\,cm^{-2}}$. If the ablation threshold is passed and the polished surface is broken the process may proceed at lower laser fluences down to $1.5\,\mathrm{J\,cm^{-2}}$.

The processed surface morphology would be of special interest among the experimental results presented in this work. Figures 5–9 show microscopic photographs of ablated crater bottoms obtained at different orientations of the treated surface. One can see a bubble structure of two micron size produced by light (figure 5). The profile of the bottom consists of a packed system of half spheres. The order observed by eye is confirmed by a corresponding diffracted signal of the probe He–Ne beam. It is interesting that the virgin place of the sample surface near the crater is packed by the same spheres. This means that two micron size balls are

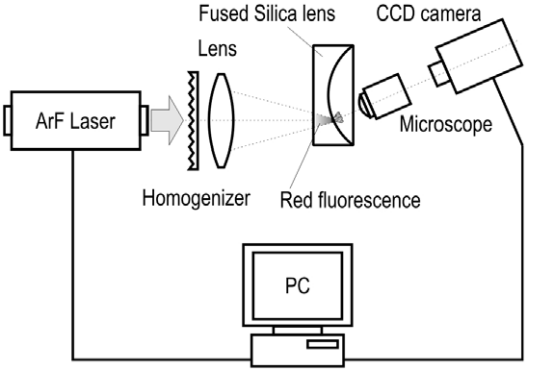

Figure 4. Experimental set-up.

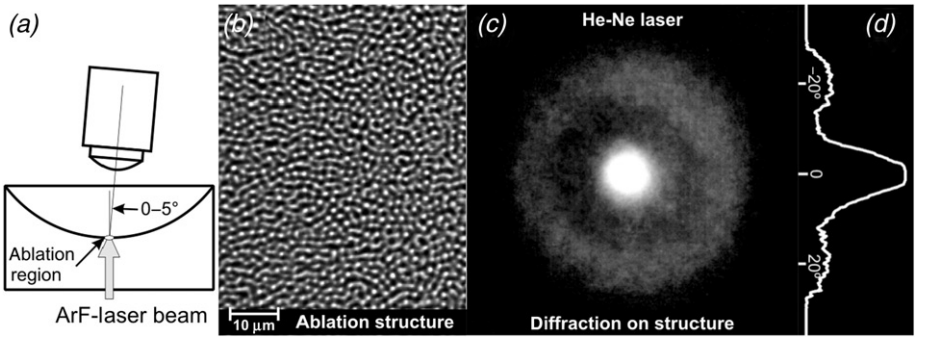

Figure 5. Profile of the treated surface after 20 ArF-laser pulses; 0° angle.

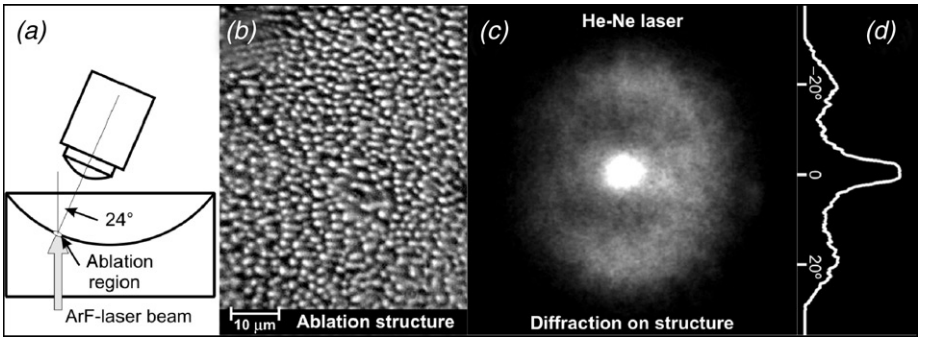

Figure 6. Same as figure 5 but angle is 24°. Spheres shown in figure 5 become ellipses.

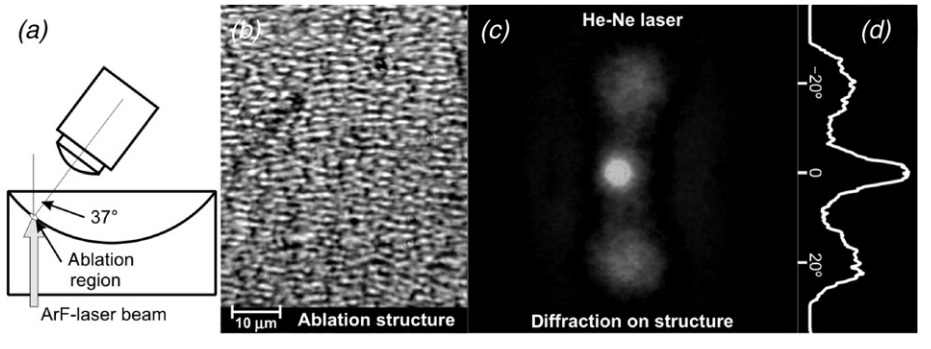

Figure 7. Same as figure 5 but angle is 37°. Ellipses become longer.

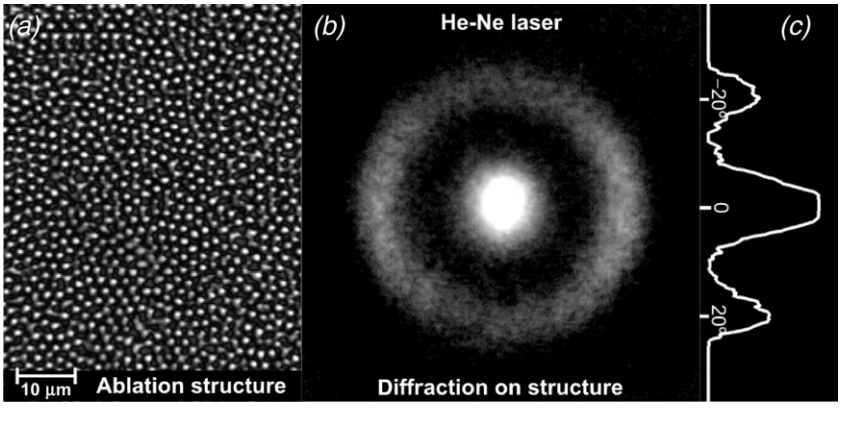

Figure 8. Profile of the treated surface after 200 ArF-laser pulses; 0° angle. Bubble structure tends to ideal with growth of the ablation crater. The corresponding angle distribution of the diffraction signal reveals narrowing.

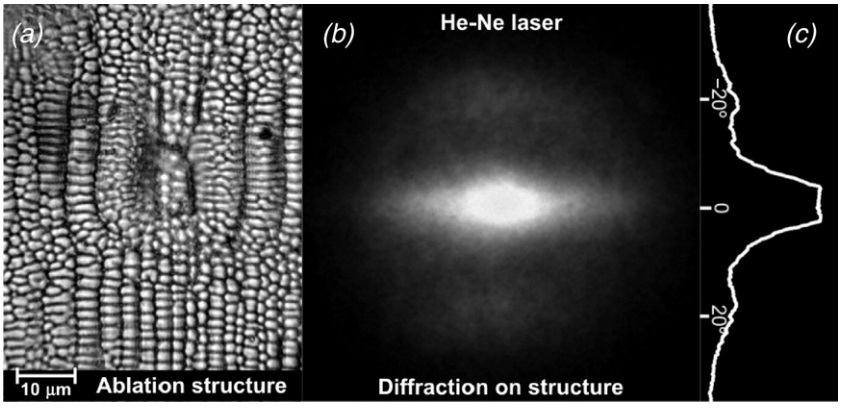

Figure 9. Combination of the ordered by light structure (horizontal direction) and self-ordered under light pumping structure (vertical direction). Light intensity is changed in horizontal direction and is constant in vertical one.

cut from the sample by the light beam and thrown out. We believe that light drives this process according to the above scenario: light driven electron bunching and subsequent local bond breaking at the boundary of the bunches where the static electric field is maximal. Light structures the matter and ablation reveals this structure. Change of the angle between the surface and the beams results in changing the spheres to ellipses (figures 6 and 7). The ablation crater depth grows proportional to the number of laser pulses passed with a rate of about 0.5 μm per pulse. It is interesting that the deeper the ablation crater the more perfect is the structure found at its bottom (figure 8). This is seen by the eye and in the narrowing of the angle distribution of the diffracted signal.

We realized one more geometry of the experiment. The fused quartz sample with plane surfaces was treated by a spacially prepared beam with high coherence in the horizontal direction (coherent length $l_c > 6$ mm) and low coherence in the vertical direction ($l_c < 10$ μm). Due to interference the light intensity structure in the horizontal direction was generated but in the vertical direction the light intensity was homogeneous. We observed organized by light and self-organized in light field structures in the same figure, i.e. figure 9 (respectively, in the horizontal and the vertical direction). In all cases the period of the self-organized structure, figures 5–9, was 2 ± 0.2 μm and coincided with periods found in our other experiments [10, 11]. The period is a characteristic of the matter but not the light and the fact confirms the self-organized nature of the ordering discussed. Analogous behaviour was observed in [13] where surface structuring took place at the SiO_2–Si interface and was explained in another way as an interface property.

One more argument in support of the scenario presented was found on performing the same experiments at longer wavelength 248 nm and comparing new behaviour with the above results for 193 nm. Theoretical estimations show that the discrepancy between the photon energy and the gap becomes too large and visualization of the structure cannot be achieved. We found that a 248 nm beam provides the ablation process but the ablation crater bottom is flat at the same fluence.

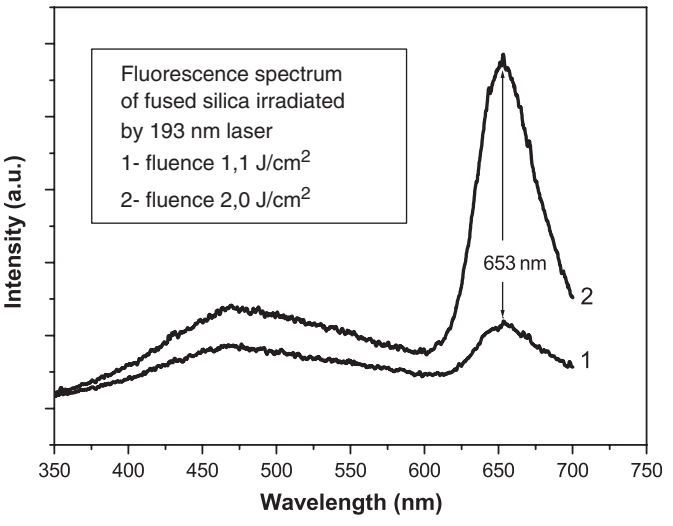

Figure 10. Red fluorescence of the UV treated sample.

As a precursor of the ablation we observed red fluorescence, as reported in numerous papers (see for example [14, 15]). It rises inside the beam channel after UV treatment and gains the maximum near the surface just before ablation. The spectrum of the red fluorescence is shown in figure 10.

4. Discussion

Our theoretical and experimental study of light driven electron kinetics in fused quartz have shown that the homogeneous distribution of the trapped electrons becomes unstable under light pumping and macroscopic electron (hole) bunches are formed. Light pushes electrons into two micron size blobs which we observed in the ablation process. The ablated crater bottom is packed by these spheres. The same packed balls are observed at the virgin surface near the crater. The last means that light cut two micron balls of the material and throws them out of the crater. It was found that a UV beam of $\lambda = 193$ nm provides bunching and subsequent local bond breaking effectively but wave $\lambda = 248$ nm cannot drive this process. Deeper electrons with short tails of electron functions are involved in this case (κ_{fi} is increased) and probabilities of the transitions are negligible. In addition, the energy discrepancy between the gap and photon energy is increased, therefore Franz–Keldysh tunnelling vanishes. We observed red luminescence of the glass sample under UV pumping before the ablation.

There are interesting investigations of the light driven structuring of a matter by femtosecond laser pulses [16–18]. The structure produced in the experiments is similar to the vertical structure of the separated furrow shown in figure 9. Authors interpreted this structuring by interference of the input beam with

generated plasmon. Indeed, the peak light power used in [16] was $2 \times 10^{14}\,\mathrm{W\,cm^{-2}}$ which exceeded considerably the pumping used in our experiment $\approx 10^{9}\,\mathrm{W\,cm^{-2}}$ and allowed one to reach high excitation necessary for plasma generation. Analogously there was an excess of light power in [17] ($\approx 10^{12}$ W in comparison with our $\approx 10^{7}$ W). Structure spaced at $\sim\lambda/2$ (determined by wavelength λ(!)) was observed and this is another peculiar feature of the structuring: spatial scale of the produced structure is given by the scale of the light field λ. At pumping above $1.2 \times 10^{13}\,\mathrm{W\,cm^{-2}}$ nonlinear memory was observed [18]. In our case the period of the structure prepared was 2 μm and does not depend on the wavelength 0.193 μm. It is determined by internal properties of the sample—electron density mainly. We can speak about light driven self-structuring in this case. According to the estimation presented in the previous section, definitely no plasma is generated in our case. The sample was put in much more soft conditions: only 10^{-5} part of the valence electrons were excited and another mechanism (not connected with plasmon) is responsible for the self-structuring observed.

Acknowledgements

This work was performed under the auspices of the Russian Academy of Sciences in the frame of the program 'Optical spectroscopy and frequency standards' and the Russian Foundation for Basic Research.

References

[1] H. Benard, Rev. Gen. Sci. Pures Appl. **12** 1261 (1900).
[2] A.N. Zaikin and A.M. Zhabotinsky, Nature **225** 535 (1970).
[3] A.M. Turing, Phil. Trans. R. Soc. London B **237** 37 (1952).
[4] F.T. Arecchi, Physica D **86** 297 (1995).
[5] B.P. Antonyuk and V.B. Antonyuk, Phys. Usp. **44** 53 (2001).
[6] B.P. Antonyuk, *Light Driven Self-organization* (Nova Science Publishers, Inc., New York, 2003).
[7] R. Kubo and Y. Toyazawa, Progr. Theor. Phys. **13** 160 (1955).
[8] W.Z. Franz, Naturforsh. Bd. **13A** 484 (1958).
[9] L.V. Keldysh, JETP **34** 1138 (1958).
[10] B.P. Antonyuk, V.B. Antonyuk, A.Z. Obidin, *et al.*, Opt. Commun. **230** 151 (2004).
[11] B.P. Antonyuk, A.Z. Obidin, S.K. Vartapetov, *et al.*, Phys. Lett. A **332** 86 (2004).
[12] K. Sugioka, J. Zhang and K. Midorikawa, Laser Machining Method and Laser Machining Apparatus, Patent No.: US 6 180 915 B1 (2001).
[13] J.J. Yu, J.V. Zhang, I.W. Boyd, *et al.*, Appl. Phys. A **72** 35 (2001).
[14] Y. Ikuta, S. Kikugawa, M. Hirano, *et al.*, Proc. SPIE **4347** 187 (2001).
[15] S.O. Kucheyev and S.G. Demos, Appl. Phys. Lett. **982** 3230 (2003).
[16] Y. Shimotsuma, P.G. Kazansky, J. Qiu, *et al.*, Phys. Rev. Lett. **91** 247405 (2003).
[17] V.R. Bhardwaj, E. Simova, P.P. Rajeev, *et al.*, Phys. Rev. Lett. **96** 057404 (2006).
[18] P.P. Rajeev, M. Gertsvolf, E. Simova, *et al.*, Phys. Rev. Lett. **97** 253001 (2006).